Available online at www.sciencedirect.com
ScienceDirect
Proceedings of the Combustion Institute 000 (2022) 1–12
Proceedings of the Combustion Institute
www.elsevier.com/locate/proci

Mass burning rate and merging behaviour of double liquid pool fires under cross winds

Fei Tang [a,*], Lei Deng [b], Qing He [c], Jianping Zhang [d,*]

[a] *State Key Laboratory of Fire Science, University of Science and Technology of China, Hefei 230026, China*
[b] *School of Emergency Management & Safety Engineering, China University of Mining & Technology, Beijing 100083, China*
[c] *School of Energy and Environment, Anhui University of Technology, Maanshan, Anhui 243002, China*
[d] *FireSERT, Belfast School of Architecture and the Built Environment, University of Ulster, Shore Road, Newtownabbey BT37 0QB, United Kingdom*

Received 1 January 2022; accepted 12 September 2022

Abstract

This paper experimentally investigates the effects of cross wind on flame interaction and burning characteristics of double liquid pool fires. Two burners were used including a square burner and a line burner. The separation distance between the double fires and the speed of cross wind were varied, providing a total of 66 test conditions. The experimental results showed that the mass burning rate increases initially with increasing separation distance until a critical value, after which the mass burning rate decreases with a further increase of the separation distance. This non-monotonic behaviour was attributed to the competition between an increase of air entrainment and a decrease of the flame heat feedback from the adjacent fire, as the separation distance increases. A correlation was developed for the mass burning rate based on the stagnant layer solution of liquid fuel evaporation and combustion, incorporating the separation distance between two fires and cross wind, and is found to predict well the experimental data for all experiments. Image analysis indicated that, with increasing separation distance, the flame merging of double pool fires can be divided into three regimes: the continuous merging regime, the intermittent merging regime, and the non-merging regime. A physical model was proposed for the flame interaction and merging behaviour of the double pool fires, based on which a piecewise function is developed for predicting the flame merging probability and the criteria for the merging/non-merging flames are also determined. The proposed formulations were found to correlate well with the current measurements of liquid pool fires and published literature data of single pool fires.

Keywords: Burning rate; Flame merging probability; Two fires; Cross winds

* Corresponding authors.
E-mail addresses: ftang@ustc.edu.cn (F. Tang), j.zhang@ulster.ac.uk (J. Zhang).

https://doi.org/10.1016/j.proci.2022.09.032

Please cite this article as: F. Tang, L. Deng, Q. He et al., Mass burning rate and merging behaviour of double liquid pool fires under cross winds, Proceedings of the Combustion Institute, https://doi.org/10.1016/j.proci.2022.09.032

1. Introduction

Following the major incidents involving pool fires that have occurred over the past decades [1,2], there has been a growing concern on pool fires safety. A typical and relevant example is the fire accident that occurred in Weifang City, China on July 2, 2000. This fire and explosion accident was caused when welding spatters created by an employee's illegal electric welding caused fuel oil vapor in tank No. 204 to explode. Fig. 1 shows an example of the fire accident in San Francisco, USA, on October 15, 2019. A fire broke out in two storage tanks of NuStar Energy LP facility in Crockett.

The fuel mass burning rate, especially under cross wind, is among the most important topics of pool fires that have been studied extensively [3–8]. Compared to the studies on the burning of a single pool fire, much less attention has been paid to the burning of multiple fires, which is usually termed as the interactively burning of two [9–16] or more [17–21] adjacent fires.

When the fuel pools are located sufficiently close to each other, the air entrainment between the fires will be restricted, which could lead flames to tilt towards each other and merge as a single flame [17–19]. The merging behaviour can have a significant impact on the burning rate. In [17], a correlation of the global burning rate of square fire arrays was proposed. Kamikawa et al. [18] studied the heights of the merged flames and the relationship between the flame height and heat release rate for multi-fire sources. Delichatsios [19] proposed a simple correlation of flame height for group fires. Vasanth et al. [20] investigated the burning rate of multiple pool fires using computational fluid dynamics (CFD) modelling, and the model was validated against the experimental data.

To better understand the flame interaction and flame radiation property, the burning rate and flame merging characteristics of multiple pool fires need to be addressed. The mass burning rate of a pool fire is determined primarily by the heat transfer to the fuel surface from the flame, which is in turn affected by the characteristic of the pool fire itself as well as external conditions such as cross air flow. Tang et al. [22] proposed a global correlation for the mass burning rate of a square acetone single pool fire by introducing a B number (fuel mass transfer number) incorporating wind speed, pool dimensions and aspect ratio. Wan et al. [23] found that in the absence of wind the burning rate and flame height of two adjacent fires change non-monotonically with the separation distance. In addition to the burning rate, the probability of flame merging of two adjacent diffusion fires is also affected by the interaction of flames as demonstrated in [16], in which correlations were proposed for the flame height of two parallel rectangular pool fires at different merging stages under no wind conditions.

Fig. 1. A fire broke out in two storage tanks, October 15, 2019, San Francisco, USA.

It should be noted that the above studies on the mass burning rate and flame characteristics are either based on a single pool fire with cross wind or two adjacent pool fires without cross wind. Flame interaction of two or more adjacent pool fires under the influence of cross wind has rarely been investigated. In a previous work [24], the authors correlated the flame tilt angle of two fires under cross wind, but have not examined the burning rate and the probability of flame merging of the double pool fires. Li et al. [25] studied the effect of cross wind on the burning behaviour of twin propane burners, which were aligned parallel to cross wind. However, as propane was used as the fuel, the fuel flow rate was pre-defined, so the interaction between the burning rate and flame heat feedback was not accounted for.

In this work, two heptane pools were used as the fuel source. Two burner dimensions were used, one square and the other representing a line burner. Different separation distances and cross wind speeds were used. Experimental results included the mass burning rate and probability of flame merging of the double pool fires. Based on the experimental data, dimensionless correlations, which incorporates the effect of separation distance and cross wind, are deduced to describe the mass burning rate and flame merging probability induced by double pool fires. The current study is aimed at improving the understanding of the interaction mechanisms of double pool fires under the effect of cross wind and providing a preliminary analytical work for further research on pool fire flame merging and experimental data for the development and validation of CFD models.

2. Experimental setup

Fig. 2 shows the experimental setup consisting of a wind tunnel 22 m (length) × 1.2 m (width) × 0.8 m (height) and two pool fires located at the downstream of the wind tunnel. A mechanical fan which can produce a maximum wind speed of 5 m/s was fixed at one end of the tunnel. In order

Please cite this article as: F. Tang, L. Deng, Q. He et al., Mass burning rate and merging behaviour of double liquid pool fires under cross winds, Proceedings of the Combustion Institute, https://doi.org/10.1016/j.proci.2022.09.032

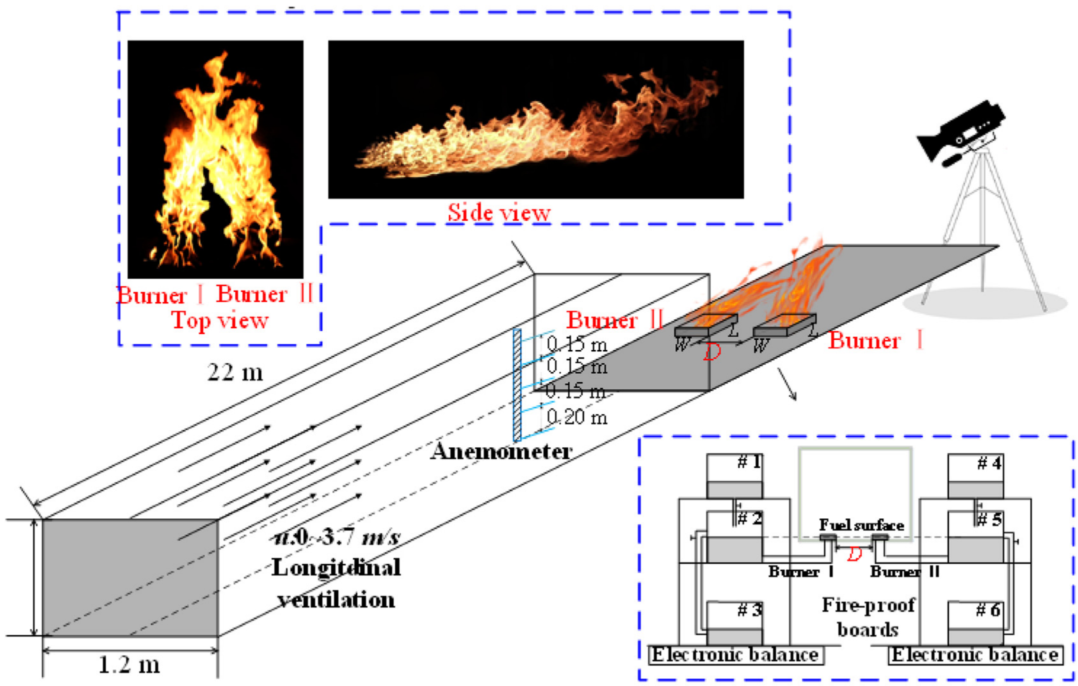

Fig. 2. Experimental setup.

to ensure a uniform air velocity, air passed through a set of honeycomb and screens before reaching the test section and a multi-channel anemometer (accuracy: 0.01 m/s) was also used to measure the wind speed at different heights. The time statistical turbulence intensity value was less than 5%. The flame shape was recorded using a CCD camera (Sony, HXR-MC88, 50 frames/second). A fireproof board (2 m × 1.2 m) was installed at the other end of the tunnel for safety. Two identical fuel pools, denoted as burnersIandII, were connected to their own liquid level stabilizers. The liquid level stabilizers were positioned in perpendicular to the air flow direction on separate fire-proof boards. Each set was placed on an electronic balance (the maximum load is 10 kg, the precision is 0.1 g, and the sampling interval is 1 s) to record the mass change of the fuel during the tests.

A total of 66 wind tunnel tests of single and two adjacent liquid pool fires were conducted. In this work, two sizes of pool burners with the same surface area but different aspect ratios were used. The burner dimensions are (square pool) and 0.474 m × 0.0474 m (line pool), rendering the burner aspect ratios (denoted as "$n = L/W$" in this paper) to be 1 and 10, respectively. The pool burner was placed 0.3 m away from the outlet portal of the wind tunnel and the pool burners were made of a 2 mm thick steel plate and have a depth of 3 cm. Heptane was selected as fuel. The initial fuel thickness was set to 2 cm, confirming to be enough to guarantee long-enough pseudo-steady burning period by a series of preliminary tests. Six speeds of cross wind (0, 1.0, 1.5, 2.0, 3.0 and 3.7 m/s) and five separation distances (0.05, 0.1, 0.2, 0.4 and 0.5 m,) were used. The ambient temperature was $303 \pm 2\ K$. Table 1 summarized the experimental conditions. Each condition was repeated three times to check repeatability, with uncertainty less than 5% based on the repeats.

3. Results and discussion

3.1. Mass burning rate of double liquid pool fires under cross wind

Fig. 3 shows a comparison of the mass burning rate of the square and line burners against the separation distance. Note that the mass burning rate presented in the figure is for one of the two pool fires. For two parallel liquid pool fires, theoretically it can be expected that the mass loss of two pool fires will the very similar as verified by the experimental data. With the increase of the separation distance, the mass burning rate increased initially until reaching a critical distance, after which the mass burning rate decreased with a further in-

Table 1
The experimental test conditions.

Test no.	Number of fires	Burner sizes, L (m) × W(m)	Cross wind, u (m/s)	Separation distance, D (m)
1–6	Single pool fire	0.15 × 0.15	0, 1, 1.5, 2, 3, 3.7	/
7–12		0.474 × 0.0474	0, 1, 1.5, 2, 3, 3.7	/
13–36	Double pool fires	0.15 × 0.15	0, 1, 1.5, 2, 3, 3.7	0.1, 0.2, 0.4, 0.5
37–66		0.474 × 0.0474	0, 1, 1.5, 2, 3, 3.7	0.05, 0.1, 0.2, 0.4, 0.5

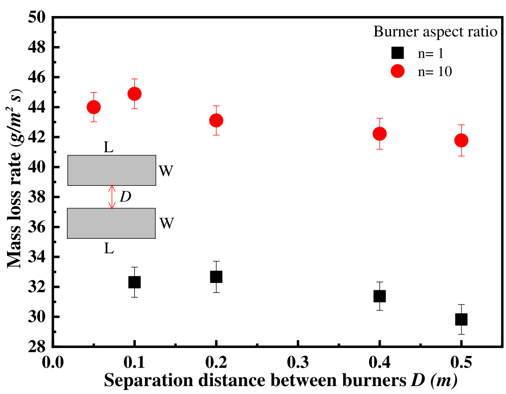

Fig. 3. Mass burning rate ($\dot{m}''$) of the steady burning stage in quiescent condition VS. Separation distance between the two adjacent pools.

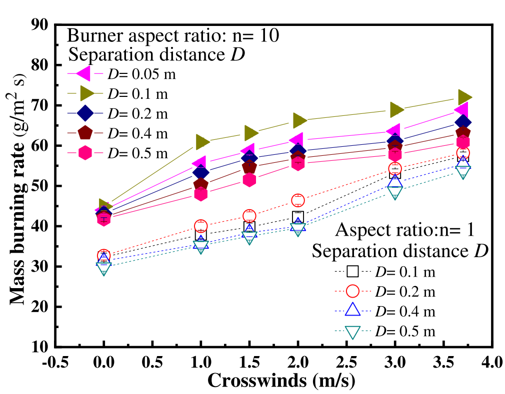

Fig. 4. Mass burning rate ($\dot{m}''$) at the steady burning stage.

crease of the separation distance. To explain this behaviour, it can be noted that as the separation distance increased, the air entrainment is increased, resulting in more burning occurs close to the fuel surface and an increased burning rate. On the other hand, the radiation heat feedback from the adjacent fire to the fuel surface will be reduced when the separation distance increases. The non-monotonic behaviour of the burning rate in Fig. 4 indicates that the two factors compete against each other. Initially, although the radiation heat feedback from the adjacent fire to the fuel surface is large, the fuel does not burn sufficiently due to the restricted entrainment. At this time, the air entrainment dominates, and the mass burning rate increases with the distance of separation of the fire source. When the separation distance is sufficiently large, an increase in the separation distance will have no further effect on air entrainment. At this time, the radiation heat feedback from the adjacent fire source to the fuel surface dominates, and the mass burning rate decreases with the increasing distance of the fire source separation.

It can also be observed in Fig. 3 that the mass burning rate for the square burner is systematically smaller than that for the line burner. This can be mainly attributed to a larger wall surface area for the line burner and, as a result, more heat conduction feedback from the flame through the side walls to the fuel than the square burner.

Fig. 4 shows the variation of the mass burning rate with increasing cross wind speed under different separation distances for both square and line burners. The uncertainty of the mass burning rate was estimated to be less than 5%. It can be noted in the figure that for the same pool size and separation distance, the mass burning rate gradually increases with the cross wind speed due to the increased supply of fresh air, but the radiation heat feedback will be reduced because of the tilting of the flames. Again, we can see clearly that the burning rate of the line burner is consistently larger than that of the square burner.

In order to further study the parallel liquid double fire, CFD simulation calculations (Fire Dynamics Simulator (FDS) (Version: 6.7.1)) are added to demonstrate the phenomenon of the flow field. For the CFD simulations, the grid size of 0.005 m was used, which is validated to be enough to capture the flow field details. The characteristics of the flow field between two adjacent fire sources (The separation distances are 0.1 m, 0.2 m, 0.4 m and 0.5 m, respectively) are analyzed, which helps us to understand some of the air entrainment considerations in our modeling process.

Fig. 5 shows the simulation results of the temperature profiles and velocity vectors of parallel double fire sources under different separation distance conditions. From the front view of the ve-

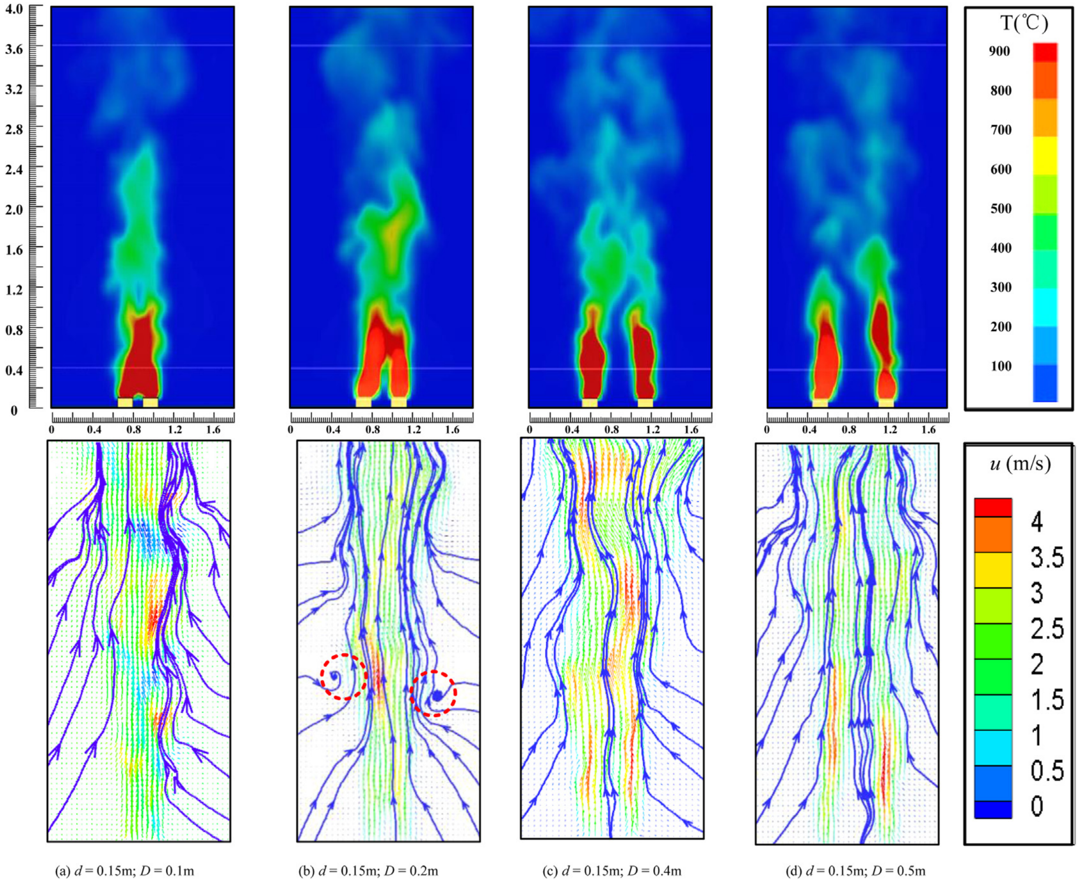

Fig. 5. CFD numerical simulation with different cross winds and fire separation distance conditions.

locity flow field shown in Fig. 5(a), it can be seen that when the separation distance is 0.1 m, the flame are completely merging, there is no air between the burners, and the air is mainly entrained from the outside of the burner. As the separation distance increases, the air entrainment from the air gap between the two flames into each flame increases.

Under cross winds, the mass flux of a single pool fire at a given radial distance from the pool centre (x) can be expressed, based on the stagnant layer solution of liquid fuel evaporation and combustion [26–28], as:

$$m''(x) = \left[\frac{k_g}{c_{pg}\delta(x)}\right]\ln(1+B) \quad (1)$$

Where $\dot{m}''$ is the mass burning rate of one of two adjacent pools fires, k_g is the gas-phase thermal conductivity, c_{pg} is the specific heat of gas phase, $\delta$is the fluid dynamical boundary layer thickness length scale, $x$is the Stream-wise distance, and B is the fuel mass transfer (Spalding) number. Its values for different fuels can be found in Arpaci and Selamet [28] (The B number for n-heptane is 5.82).

According to the boundary layer flow theory [29]:

$$\frac{\delta}{x} \sim \frac{1}{\mathrm{Re}_x^{\lambda}} \quad (2)$$

Where the exponent λ=1/2 for laminar flows and approximately 4/5 for turbulent flows [30]. For forced convection, $\mathrm{Re}_x = ux/v$, where v is the kinematic viscosity, Re is the Reynolds number, and u is the cross wind speed, thus we have

$$\frac{\delta}{x} \sim \frac{1}{\mathrm{Re}_x^{1/2}} \sim \left(\frac{v}{ux}\right)^{1/2} \quad (3)$$

Substituting Eq. (3) into Eq. (1) and integrating along the hydrocarbon fuel pool from the centre to the edge (D_h) yields

$$\dot{m}'' = \frac{1}{D_h}\int_0^{\frac{D_h}{2}} \dot{m}''(x)dx \quad (4)$$

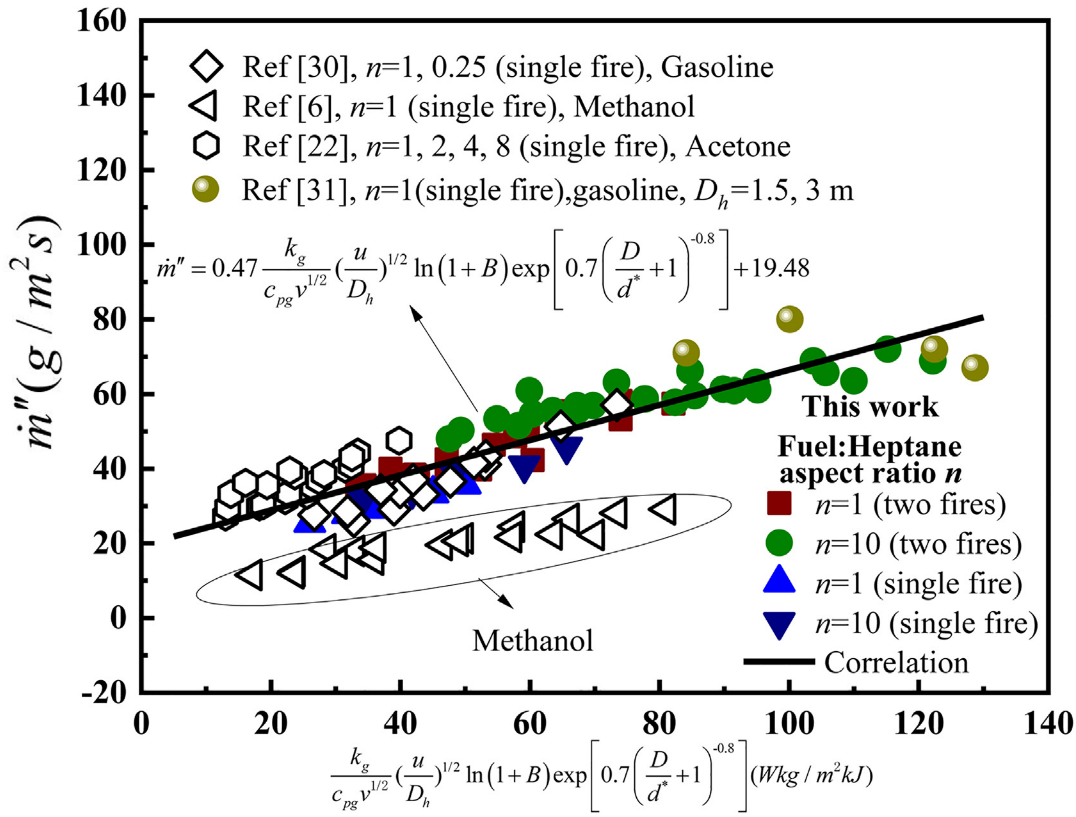

Fig. 6. Scaling of mass burning rate based on stagnant layer theory and fuel mass transfer number in cross wind ($u > 0$).

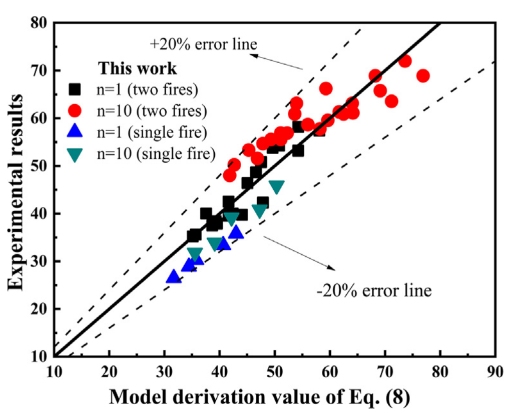

Fig. 7. Comparison of the mass burning rate predicted by the proposed correlation (Eq. (8)) and the experimental results.

Where D_h is the hydraulic diameter of a pool ($D_h = 4LW/2(L + W)$). Combining Eqs. (1) and (4), one obtains:

$$\dot{m}'' \propto \frac{k_g}{c_{pg}\nu^{1/2}}\left(\frac{u}{D_h}\right)^{1/2}\ln(1+B) \tag{5}$$

Fig. 4 indicates that the mass burning rate of two adjacent pool fires for a given cross wind speed depends on the separation distance D. We introduce here a new dimensionless parameter (D/d^*) (where $d^*$is the characteristic perimeter diameter of the pool, ($d^*=2(L+W)/\pi$)), to incorporate the effect of the separation distance on the combined mass burning rate based on the stagnation layer solution theory of a single pool fire source under relatively strong air convection:

$$\dot{m}'' = fcn\left[\frac{k_g}{c_{pg}\nu^{1/2}}\left(\frac{u}{D_h}\right)^{1/2}\ln(1+B), \frac{D}{d^*}\right] \tag{6}$$

According to the overall trend of mass loss rate with the fire separation distance, the following function is proposed to incorporate the effect of cross air flow, burner separation distance and burner aspect ratio on the mass burning rate of two adjacent pool fires.

$$\dot{m}'' \propto \frac{k_g}{c_{pg}\nu^{1/2}}\left(\frac{u}{D_h}\right)^{1/2}\ln(1+B)\exp\left[\alpha\left(\frac{D}{d^*}+1\right)^{-\beta}\right] \tag{7}$$

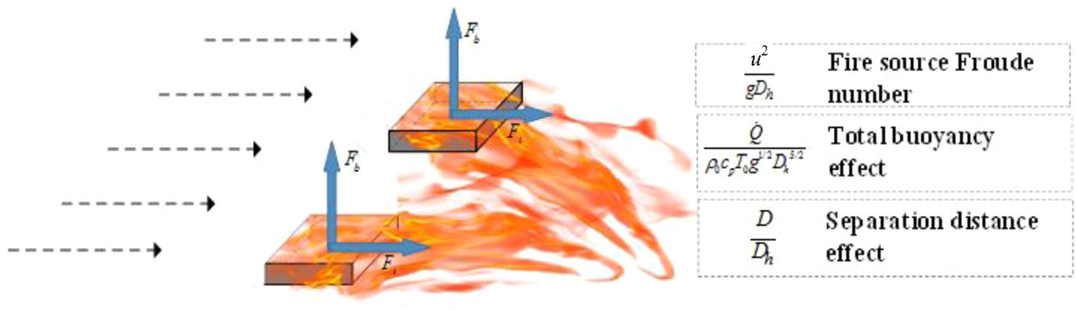

Fig. 8. A physical model for flame interaction of double liquid pool fires under cross winds.

where $\alpha$and β are constants which were determined based on the best fitting of the data as shown in Fig. 6, having values of 0.7 and 0.8, respectively.

$$\dot{m}'' = 0.47\frac{k_g}{c_{pg}\nu^{1/2}}\left(\frac{u}{D_h}\right)^{1/2}\ln(1+B)\exp\left[0.7\left(\frac{D}{d^*}+1\right)^{-0.8}\right]+19.48 \quad (8)$$

Eq. (8) was obtained using the data of this study and that in the literature [6,22,30,31]. The new correlation captures well the mass burning rate of the gasoline [30,31] and acetone fires [22]. Meanwhile, the correlation proposed in this paper can better characterize the large-scale experimental data [31]. However, it overpredicts the mass burning rate of the methanol fire [6]. This could be explained by the fact that a methanol fire is much less sooty than the other fuels considered here and thus the radiative heat feedback from the flame to the fuel surface would hence be less comparing with other hydrocarbon flames. The constant of proportionality derived from the heptane data in the present study would hence lead to overpredictions of radiative heat feedback to the fuel surface and, as a result, the fuel evaporation rate. Fig. 7 shows the comparison of the experimentally measured data (for both single and double pool fires) in this study with those predicted by the proposed correlation (Eq. (8)). There is a good agreement between the two sets of data with a relative error less than 20%. Note that in the calculations the burning of the single fire was considered to be equivalent to that of the double fires whose separation distance is infinite (∞).

3.2. Flame merging behaviour of double liquid pool fires under cross wind

3.2.1. Theoretical analysis

In order to predict the flame merging behaviour of the double liquid pool fires, it is important to examine the underlying physical phenomena in such a configuration. Fig. 8 presents a physical model for flame interaction of double pool fires under cross wind. As can be seen from the figure, the main factors affecting the flame merging are:

(a) The inertia force (*Fi*) induced by cross wind: as the cross wind increases, the air exchange between the two burners accelerates and the air entrainment increases from the air gap between the two flames into each flame, thus increasing the burning rate of the liquid. At the same time, this leads to a decrease in the pressure ratio between the outer left and right sides and the two burners, which leads to a decrease in the probability of flame merging.
(b) The thermal buoyancy (*Fb*) induced by flame burning: thermal buoyancy depends mainly on the fire heat release rate. As the fire heat release rate increases, the flame merging probability increases.
(c) The separation distance effect *D*/*Dh*: as the separation distance increases, the heat feedback received by the liquid decreases, which leads to a decrease in the liquid burning rate. Also, the flame merging probability decreases.

3.2.2. Physical modeling of flame merging in a two-liquid pool fire under cross winds

As we discussed earlier, the merging behaviour of two adjacent fires depends on both the separation distance and cross wind speed. This is clearly demonstrated in Fig. 9, showing typical images of the two parallel rectangular flames from the line burner. Fig. 9(a) depicts the merging behaviour of the double pool fires as the separation distance increases under no wind, whereas Fig. 9(b) shows the merging behaviour as the wind speed increases for the same separation distance ($D = 0.2$ m).

Analysis of the images in Fig. 9 reveals that the flame merging characteristics of double pool fires can be divided into three regimes with increasing

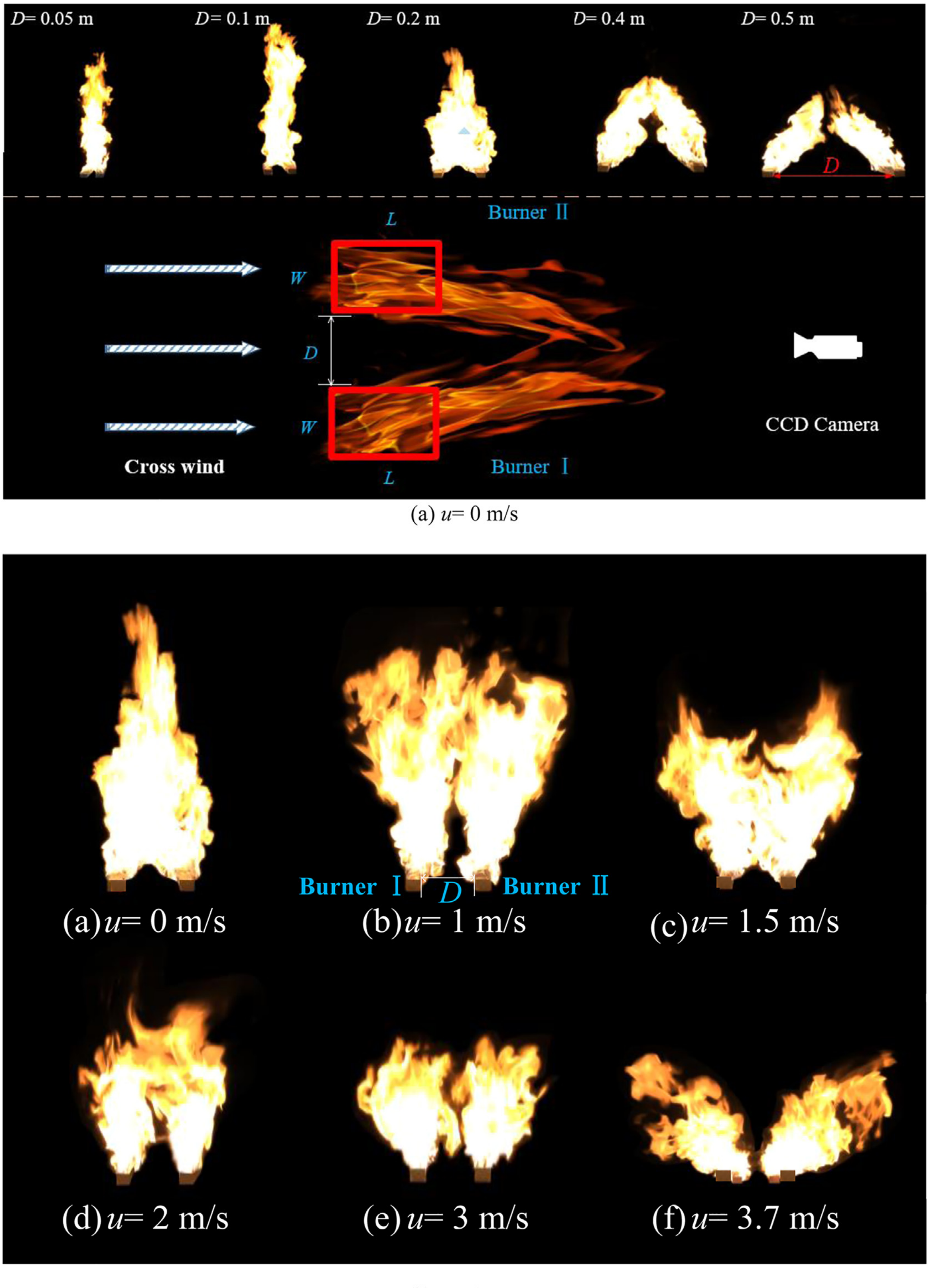

Fig. 9. Flame morphology relationship between two parallel rectangular fires (Front view), aspect ratio $n = 10$.

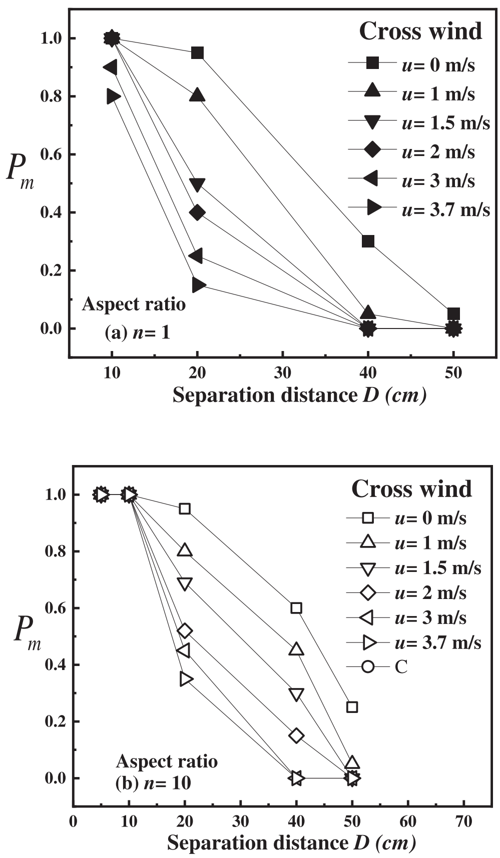

Fig. 10. Flame merging probability P_m against separation distance D.

separation distance D: (1) the continuous merging regime; (2) the intermittent merging regime, and (3) the non-merging regime, where the flames burn independently.

Based on the image processing method of flame merging [32], we can introduce the flame merging probability of double pool fires under cross wind. Flame merging probability P_m is defined as the number of frames showing flame merging N_m divided by the total number of frames N within 60 s during the steady burning state.

$$P_m = \frac{N_m}{N} \tag{9}$$

If the flames burn independently, $P_m = 0$, if the two fires always merge, $P_m = 1$, and $0 < P_m < 1$ corresponds to the intermittent flame merging regime.

Fig. 10 shows the evolution of flame merging probability with the burner separation distance for both square and line burners. We can observe that (a) for all the cases, the flame merging probability P_m decreases from 1 to 0 with increasing separation distance D, and (b) for the cases with the same separation distance, the flame merging probability P_m generally decreases with increasing cross wind speed. Clearly, the characteristics of the pool fire ($\dot{Q}$, D_h, D), ambient parameters (ρ_0, C_p, T_0, g) and the cross wind speed u are the controlling parameters for determining P_m, i.e.,

$$P_m = fcn\left(\dot{Q}, \rho_0, c_p, T_0, g, u, D, D_h\right) \tag{10}$$

Where the chemical heat release rate can be calculated as

$$\dot{Q} = \chi \dot{m}'' \Delta H_c \tag{11}$$

where χ is the combustion efficiency and ΔH_c is the heat of combustion per unit fuel mass, which is 44.56 MJ/kg for n-heptane.

Based on dimensional analysis, Eq. (10) can be re-written as:

$$P_m = fcn\left(\frac{\dot{Q}}{\rho_0 c_p T_0 g^{1/2} D_h^{5/2}}, \frac{u^2}{gD_h}, \frac{D}{D_h}\right) \tag{12}$$

Based on above dimensional analysis, we correlated the flame merging probability P_m with dimensionless fire heat release rate $\dot{Q}^* = \dot{Q}/(\rho_0 c_p T_0 g^{1/2} D_h^{5/2})$, Froude number and dimensionless separation distance D/D_h, as shown in Fig. 11. A piecewise function can be deduced as shown in Eq. (13), which represents the "fully merging regime", the "intermittent merging regime", and the "non-merging regime", respectively. It can also be noted that the proposed correlation also predicts well the experimental data in a previous study [12] for two parallel rectangular fires under no wind.

$$P_m = \begin{cases} 1, \\ \dot{Q}^{*-0.95}\left(\frac{u^2}{gD_h} + 0.5\right)^{1/3}\left(\frac{D}{D_h}\right)^{0.6} \le 0.09 \\ 1.7 - 7.74\dot{Q}^{*-0.95}\left(\frac{u^2}{gD_h} + 0.5\right)^{1/3}\left(\frac{D}{D_h}\right)^{0.6}, \\ 0.09 < \dot{Q}^{*-0.95}\left(\frac{u^2}{gD_h} + 0.5\right)^{1/3}\left(\frac{D}{D_h}\right)^{0.6} \le 0.22 \\ 0, \\ \dot{Q}^{*-0.95}\left(\frac{u^2}{gD_h} + 0.5\right)^{1/3}\left(\frac{D}{D_h}\right)^{0.6} > 0.22 \end{cases} \tag{13}$$

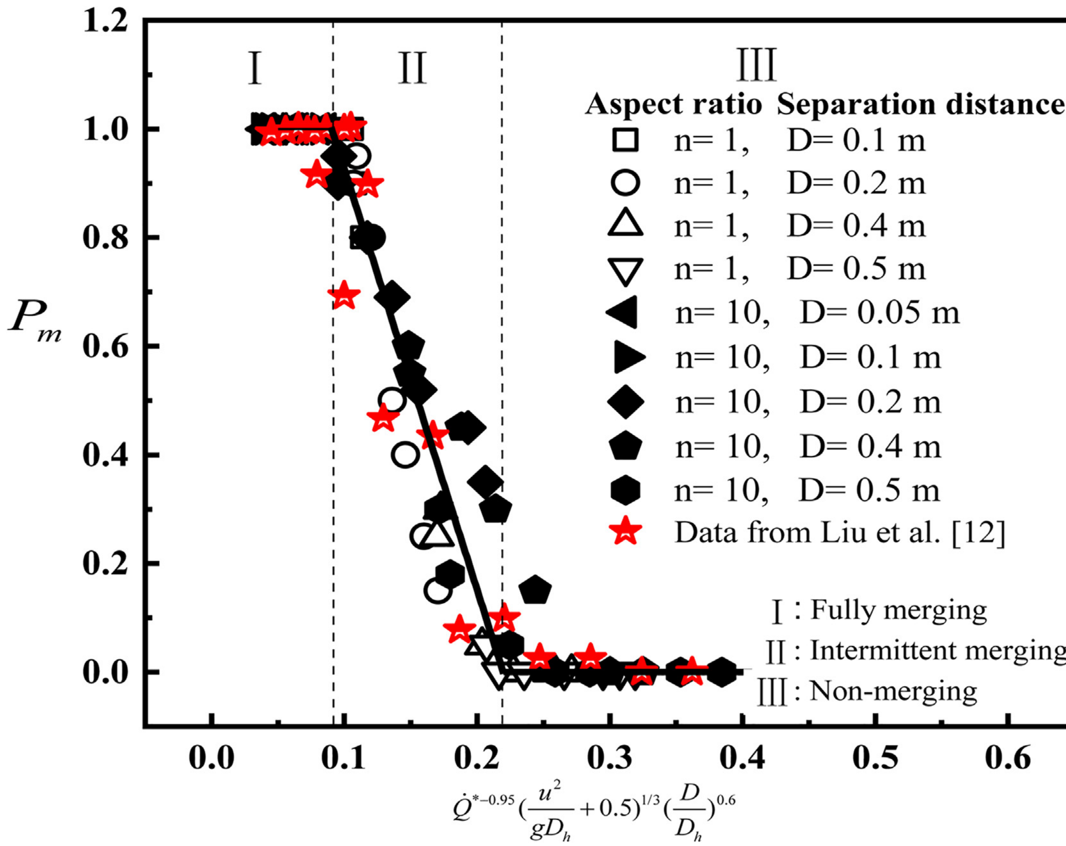

Fig. 11. Flame merging probability P_m against dimensionless heat release rate, Froude number and separation distance D.

4. Conclusions

In this paper, experimental and theoretical work was conducted to study the mass burning rate and flame merging behaviour of double liquid pool fires under cross wind. Two burner aspect ratios, six cross wind speeds and five separation distances (between the two pool fires) were used. The major findings are as follows:

(1) The mass burning rate of two adjacent pool fires was found to exhibit a non-monotonic behaviour. It increases initially with the separation distance until a critical value, after which it decreases with a further increase in the separation distance. This was attributed to the fact that, with increasing cross wind speed, air entrainment increases whereas the radiation feedback from the adjacent fire decreases. These two factors compete against each and dominate depending on the separation distance. A correlation was developed for the mass burning rate based on the stagnant layer solution of liquid fuel evaporation and combustion, incorporating the separation distance between two fires and cross winds. The deduced correlation predicts well the present experimental data for heptane as well as the literature data for gasoline and acetone for both double and single pool fires, with the distance set to infinite for the latter.

(2) The flame merging characteristics were examined by imaging analysis. Three regimes were identified with increasing separation distance and cross wind, fully merging, intermittent merging and non-merging, applicable to all experimental data. Based on dimensional analysis, a piecewise linear function for the flame merging probability was developed (Eq. (13)), which correlates well with the present data and that in the literature for two parallel fires under no cross wind.

Declaration of Competing Interest

The authors declare there are no conflicts of interest regarding the publication of this paper.

Please cite this article as: F. Tang, L. Deng, Q. He et al., Mass burning rate and merging behaviour of double liquid pool fires under cross winds, Proceedings of the Combustion Institute, https://doi.org/10.1016/j.proci.2022.09.032

Acknowledgments

This work was supported by National Natural Science Foundation of China under Grant No. 52076066, CAS Pioneer Hundred Talents Program to Dr. Fei Tang, Anhui Provincial Natural Science Foundation (No. 2208085J34), High-end Foreign Experts Introduction Plan Project and Leading Academic Talents Training Program of USTC to Dr. Fei Tang.

References

[1] S. Vasanth, S.M. Tauseef, T. Abbasi, S.A. Abbasi, Multiple pool fires: occurrence, simulation, modeling and management, J. Loss Prev. Process 29 (2014) 103–121.
[2] C.S. Lam, E.J. Weckman, Wind-blown pool fire, part II: comparison of measured flame geometry with semi-empirical correlations, Fire Saf. J. 78 (2015) 130–141.
[3] V. Babrauskas, Estimating large pool fire burning rates, Fire Technol. 19 (1983) 251–261.
[4] J.M. Chatris, J. Quintela, J. Folch, E. Planas, J. Arnaldos, J. Casal, Experimental study of burning rate in hydrocarbon pool fires, Combust. Flame 126 (1) (2001) 1373–1383.
[5] F. Ferrero, M. Munoz, B. Kozanoglu, J. Casal, J. Arnaldos, Experimental study of thin-layer boilover in large-scale pool fires, J. Hazard. Mater. 137 (3) (2006) 1293–1302.
[6] J. Woods, B. Fleck, L. Kostiuk, Effects of transverse air flow on burning rates of rectangular methanol pool fires, Combust. Flame 146 (2006) 379–390.
[7] D.D. Benjamin, R.L. John de, K.B. Thomas, C. Marcos, G. Robert, B.D. Sergey, Pool fires – an empirical correlation, Combust. Flame 160 (12) (2013) 2964–2974.
[8] R.M. Leite, F.R. Centeno, Effect of tank diameter on thermal behavior of gasoline and diesel storage tanks fires, J. Hazard. Mater. 342 (2018) 544–552.
[9] C.F. Tao, Q.P. Ye, J.J Wei, Q. Shi, F. Tang, Experimental study on Flame–Flame interaction and its merging features induced by double rectangular propane diffusion burners with various aspect ratios, Combust. Sci. Technol. 191 (8) (2019) 1416–1429, doi:10.1080/00102202.2018.1529031.
[10] K. Kuwana, S. Kato, A. Kosugi, T. Hirasawa, Y. Nakamura, Experimental and theoretical study on the interaction between two identical micro-slot diffusion flames: burner pitch effects, Combust. Flame 165 (2016) 346–353.
[11] L.H. Hu, L.L. Huang, Q. Wang, K. Kuwana, Experimental study and analysis on the interaction between two slot-burner buoyant turbulent diffusion flames at various burner pitches, Combust. Flame 186 (2017) 105–113.
[12] N.A. Liu, S.J. Zhang, X.S. Luo, J. Lei, H.X. Chen, X.D. Xie, L.H. Zhang, R. Tu, Interaction of two parallel rectangular fires, Proc. Combust. Inst. 37 (2019) 3833–3841.
[13] L. Deng, F. Tang, P. Hu, Physical modeling and machine learning of ceiling maximum temperature rise induced by tandem heat sources with unequal heat release rates in a natural ventilation tunnel, Int. J. Heat Mass Transf. 197 (2022) 123333.
[14] Q. Wang, S.M. Wang, H. Liu, J.Y. Shen, F.J. Shang, C.L. Shi, F. Tang, Characterization of ceiling smoke temperature profile and maximum temperature rise induced by double fires in a natural ventilation tunnel, Tunn. Undergr. Space Technol. 96 (2020) 103233.
[15] Y.H. Chen, L.H. Hu, C. Kuang, X.L. Zhang, Y.J. Lin, X.P. Zhong, Flame interaction and tilting behavior of two tandem adjacent hydrocarbon turbulent diffusion flames in crosswind: an experimental quantification and characterization, Fuel 290 (2021) 119930.
[16] K.Y. Li, Z.Z. Ma, X.Y. Huang, Y.Y. Zou, Merging dynamics of dual parallel linear diffusion flames, Fire Saf. J. 127 (2022) 103490.
[17] N.A. Liu, Q. Liu, J.S. Lozano, L.F. Shu, L.H. Zhang, J.P. Zhu, Z.H. Deng, K. Satoh, Global burning rate of square fire arrays: experimental correlation and interpretation, Proc. Combust. Inst. 32 (2009) 2519–2526.
[18] D. Kamikawa, W.G. Weng, K. Kagiya, Y. Fukuda, R. Mase, Y. Hasemi, Experimental study of merged flames from multifire sources in propane and wood crib burners, Combust. Flame 142 (2005) 17–23.
[19] M.A. Delichatsios, A correlation for the flame height in "group" fires, Fire Sci. Technol. 26 (2007) 1–8.
[20] S. Vasanth, S.M. Tauseef, T. Abbasi, A.S. Rangwala, S.A. Abbasi, Assessment of the effect of pool size on burning rates of multiple pool fires using CFD, J. Loss Prev. Proc. 30 (2014) 86–94.
[21] W.G. Weng, D. Kamikawa, Y. Hasemi, Experimental study on merged flame characteristics from multifire sources with wood cribs, Proc. Combust. Inst. 35 (2015) 2597–2606.
[22] F. Tang, L.J. Li, K.J. Zhu, Z.W. Qiu, C.F. Tao, Experimental study and global correlation on burning rates and flame tilt characteristics of acetone pool fires under cross air flow, Int. J. Heat Mass Transf. 87 (2015) 369–375.
[23] H.X. Wan, Z.H. Gao, J. Ji, Y.M. Zhang, K.Y. Li, L.Z. Wang, Effects of pool size and sepration distance on burning rate and flame height of two square heptane pool fires, J. Hazard. Mater. 369 (2019) 116–124.
[24] C.G. Fan, F. Tang, Flame interaction and burning characteristics of abreast liquid fuel fires with cross wind, Exp. Therm. Fluid Sci. 82 (2017) 160–165.
[25] B. Li, H.X. Wan, Z.H. Gao, J. Ji, Experimental study on the characteristics of flame merging and tilt angle from twin propane burners under cross wind, Energy 174 (2019) 1200–1209.
[26] J.L. de Ris, L. Orloff, A dimensionless correlation of pool burning data, Combust. Flame 18 (1972) 381–388.
[27] J.G. Quintiere, Diffusive burning of liquid fuels, Fundamentals in Fire Phenomenon, John Wiley & Sons Ltd, 2006.
[28] V.S. Arpaci, A. Selamet, Buoyancy-driven turbulent diffusion flames, Combust. Flame 86 (1991) 203–215.
[29] A.V. Singh, M.J. Gollner, Estimation of local s burning rates for steady laminar boundary layer diffusion flames, Proc. Combust. Inst. 35 (2015) 2527–2534.
[30] L.H. Hu, S. Liu, Y. Xu, D. Li, A wind tunnel experimental study on burning rate enhancement behavior of gasoline pool fires by cross air flow, Combust. Flame 158 (2011) 586–591.

[31] J. Lei, W.Y. Deng, Z.H. Liu, S.H. Mao, K. Saito, Y. Tao, H.M. Wu, C.L. Xie, Experimental study on burning rates of large-scale hydrocarbon pool fires under controlled wind conditions, Fire Saf. J. 127 (2022) 103517.

[32] K.H. Lu, L.H. Hu, M. Delichatsios, F. Tang, Z.W. Qiu, L.H. He, Merging behavior of facade flames ejected from two windows of an under-ventilated compartment fire, Proc. Combust. Inst. 35 (2015) 2615–2622.

Please cite this article as: F. Tang, L. Deng, Q. He et al., Mass burning rate and merging behaviour of double liquid pool fires under cross winds, Proceedings of the Combustion Institute, https://doi.org/10.1016/j.proci.2022.09.032